

Quantum phase transitions in trimerized zigzag spin ladders

H. D. Rosales,¹ D. C. Cabra,^{1,2,3} M. D. Grynberg,¹ G. L. Rossini,¹ and T. Vekua^{2,4}

¹*Departamento de Física, Universidad Nacional de La Plata, C.C. 67, 1900 La Plata, Argentina*

²*Laboratoire de Physique Théorique, Université Louis Pasteur, 3 Rue de l'Université, 67084 Strasbourg, Cédex, France*

³*Facultad de Ingeniería, Universidad Nacional de Lomas de Zamora, Cno. de Cintura y Juan XXIII, 1832 Lomas de Zamora, Argentina*

⁴*Laboratoire de Physique Théorique et Modèles Statistiques, Université Paris Sud, 91405 Orsay Cedex, France*

(Received 13 December 2006; revised manuscript received 6 March 2007; published 31 May 2007)

We analyze the effects of a trimerized modulation in a quantum spin $S=\frac{1}{2}$ zigzag ladder at the magnetization plateau $M=1/3$. Such periodicity is argued to be stemmed from lattice deformations by phonons. The interplay between frustration and exchange modulation is well described by an effective triple sine-Gordon field theory close to the homogeneous ladder and by block-spin perturbation theory in the weakly coupled trimer regime. The characteristic triple degeneracy of the ground state for homogeneous ladders gives place to modulation driven quantum phase transitions, leading to a rich phase diagram including up-up-down, quantum plateau, and gapless plateau states.

DOI: [10.1103/PhysRevB.75.174446](https://doi.org/10.1103/PhysRevB.75.174446)

PACS number(s): 75.10.Jm, 73.43.Nq, 75.30.-m

I. INTRODUCTION

Frustrated quasi-one-dimensional antiferromagnetic spin $S=\frac{1}{2}$ systems have been extensively studied in the last years. One of the most discussed and paradigmatic models is the J_1 - J_2 zigzag ladder, which, apart from the theoretical interest caused by the frustration, is believed to be the relevant starting point for describing magnetic excitations of a number of real quasi-one-dimensional materials.¹ Among others, attention is focused on CuGeO_3 where, along with frustration, spontaneous spin-Peierls exchange modulation caused by the coupling between spins and phonons plays a crucial role.² Due to the interest in the above material, the interplay between exchange modulation and frustration has stimulated considerable efforts in purely spin systems as well, with studies concentrating on the zero magnetization case.³⁻⁷

Recently, it was shown that phonons in frustrated zigzag ladders can open plateaus not only at zero magnetization but at other rational values M of saturation ($M=1/3, 1/2, \dots$).⁸ Spontaneous exchange modulations in such situations could also take place, with a spatial pattern associated with the (generally broken) ground-state translational symmetry.

In this work, we will concentrate on the interplay between exchange modulation and frustration in a pure zigzag spin ladder at the $M=1/3$ plateau state. This system, in the absence of modulation, is known to exhibit a magnetization plateau when the next-nearest-neighbor (NNN) coupling J_2 is large enough with respect to the nearest-neighbor (NN) coupling J_1 .^{9,10} Moreover, the ground state is threefold degenerate and translation symmetry by one lattice spacing is spontaneously broken to an up-up-down configuration.⁹ A natural elastic deformation is then given by a period three pattern

$$u_i = \delta \sin\left(\frac{2\pi}{3}i - \Phi_0\right), \quad (1)$$

where u_i is a relevant scalar coordinate describing the displacement of the i th ion sequentially numbered on a one-dimensional chain. We will pay attention to the most symmetric situation $J_1=J_2$ and a deformation with amplitude δ

>0 and phase $\Phi_0=-\frac{\pi}{3}$ that causes sites 1 and 3 to move closer to site 2 and so on. We assume that magnetic exchange couplings vary linearly with the relative displacement to estimate the modulation on both NN and NNN couplings. In this way, sites 1, 2, and 3 are magnetically coupled by equally enhanced exchanges $J=J_1+\lambda$ forming *equilateral triangular trimers* as shown in Fig. 1. Couplings drawn with dashed lines are weaker than J_1 , which, for simplicity, we represent as $J'=J_1-\lambda$.

Notice that this deformation selects triangles with stronger couplings as basic frustrated units, with weaker couplings between them; in a limiting situation that we will also consider, the system is formed by weakly coupled triangular trimers where strong frustration enhances plateau formation and directly relates to high degeneracy of the ground state. On the other hand, a deformation with $\delta<0$ (stronger couplings along dashed lines in Fig. 1) modifies the system toward a single homogeneous spin chain with modulated weaker couplings between non-NN, up to fourth neighbors; the corresponding limiting situation ($J/J'=0$) is just a usual spin chain running along the dashed line, where no plateau would be observed in the magnetization curve.

Guided by this quick analysis, in the present paper, we will investigate the $M=1/3$ ground state of the trimerized antiferromagnetic spin $S=\frac{1}{2}$ zigzag ladder. Specifically, we start with a homogeneous Heisenberg antiferromagnetic zigzag ladder with exchanges $J_1=J_2$ at $1/3$ magnetization. This situation is well above the critical coupling $J_2=0.487J_1$,¹¹ so that the system exhibits the magnetization plateau with a

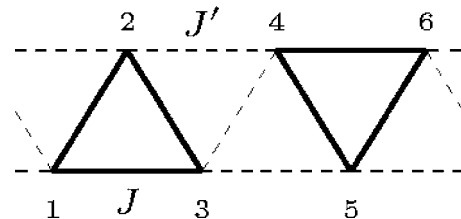


FIG. 1. Schematic description of the trimerized zigzag spin ladder. Both nearest and next-nearest couplings are modulated.

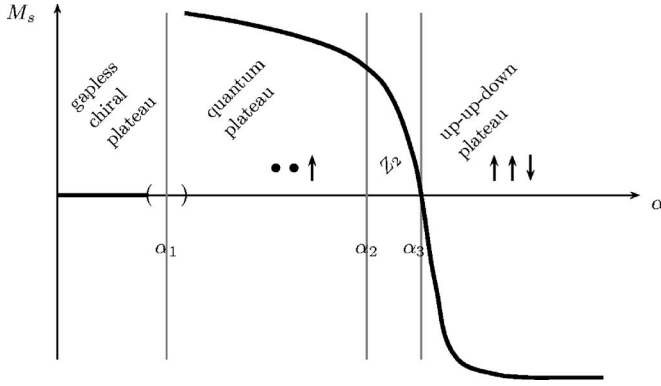


FIG. 2. Schematic description of the ground-state phase diagram of the spin system shown in Fig. 1. M_s is a magnetization order parameter to be referred to in Eq. (22).

threefold degenerate ground state. We then consider a lattice deformation of period 3, giving rise to a modulation of the same order on NN and NNN exchange couplings. The Hamiltonian can be written as

$$H = \sum_i (J_i \vec{S}_i \cdot \vec{S}_{i+1} + \tilde{J}_i \vec{S}_i \cdot \vec{S}_{i+2}), \quad (2)$$

where \vec{S}_i denotes a spin $\frac{1}{2}$ operator at site i . The modulation is given by NN antiferromagnetic couplings $J_i > 0$ forming a sequence of period 3 with $J_1 = J_2 = J$, $J_3 = J'$, and NNN antiferromagnetic couplings $\tilde{J}_i > 0$ also forming a sequence of period 3 with $\tilde{J}_1 = J$, $\tilde{J}_2 = \tilde{J}_3 = J'$.

As we will see, the interplay between frustration and modulation gives rise to a very rich ground-state phase diagram involving a number of quantum phase transitions of different orders, including up-up-down, quantum plateau, and gapless chiral plateau states. In summary, our analysis will show that the system adopts a unique up-up-down ground state for $\alpha \equiv J'/J > 1$ separated by a first-order transition at $\alpha_3 = 1$ from a Z_2 degenerate ground-state phase extending to α slightly less than 1. At some finite distance $\alpha_2 < 1$, we find a second-order transition of Ising class to a unique quantum plateau state. These quantum phase transitions should be contrasted with the stability of the threefold degenerate ground state against translation invariant modifications of the zigzag couplings J_1, J_2 .⁹ Toward the strong frustration regime $\alpha \ll 1$, we find another transition at $0 < \alpha_1 < \alpha_2$ to a gapless chiral phase with uniform magnetization ground state. Thus, we provide a phase diagram with J' starting from zero (decoupled triangular trimers) up to $J' > J$, schematically shown in Fig. 2. The analysis relies on bosonization, renormalization group, and block-spin perturbations, supported by numerical diagonalization on finite-size systems. A detailed knowledge of these transitions will ultimately help understand the possibility of spin-Peierls-like phenomenon in magnetized materials.

The paper is organized as follows. In Sec. II, we study the regime of weak modulation $J' \sim J$ by bosonization, obtaining a triple sine-Gordon effective theory. In Sec. III, we study the strong frustration regime, where block-spin perturbation theory is applicable. Effective Hamiltonians at first and sec-

ond orders are analyzed. In Sec. IV, we study numerically the ground state and low-lying excitations in finite systems by exact diagonalization; this supports the semiquantitative bosonization results and provides a bridge between weak modulation and strong frustration regimes. In Sec. V, we present our conclusions and prospects for future work.

II. WEAKLY MODULATED SYSTEMS

We first analyze the stability of the zigzag ladder plateau ground state at $M = 1/3$ against small modulated perturbations, as defined in Eq. (2) for $J' \sim J$. The microscopic Hamiltonian for the system can be conveniently written as

$$H = \sum_i \left[\left(J - \frac{\epsilon}{2} \right) \vec{S}_i \cdot \vec{S}_{i+1} + (J - \epsilon) \vec{S}_i \cdot \vec{S}_{i+2} - h S_i^z \right] - \epsilon \sum_i \cos\left(i \frac{2\pi}{3}\right) \vec{S}_i \cdot \vec{S}_{i+1} + \epsilon \sum_i \cos\left((i-1) \frac{2\pi}{3}\right) \vec{S}_i \cdot \vec{S}_{i+2}, \quad (3)$$

where $\epsilon = 2(J - J')/3$. The first line describes a homogeneous zigzag ladder with $J_1 = J - \epsilon/2$ and $J_2 = J - \epsilon$ in an external magnetic field h , while the rest is a modulated perturbation of period 3.

Once the magnetic field is tuned to the plateau range, the homogeneous part is well described^{10,12} by bosonization with an effective massive sine-Gordon Hamiltonian

$$H_0 = \frac{v}{2} \int dx \left[\frac{1}{K} (\partial_x \phi)^2 + K (\partial_x \tilde{\phi})^2 \right] - g \cos(3\sqrt{4\pi}\phi), \quad (4)$$

where ϕ is a real bosonic field with spin-wave velocity v and compactification radius $R = 1/\sqrt{4\pi}$,²⁸ and $\tilde{\phi}$ is its dual field defined by $\partial_x \tilde{\phi} = \partial_x \phi$. The Luttinger parameter K takes into account renormalization due to spin interactions. The presence of the third harmonic of the bosonic field arises from a triple Umklapp term, only allowed at the Fermi momentum $k_F = \pi/3$ fixed by the magnetization $M = 1/3$. Moreover, K has to be sufficiently small, $K < 2/9$, rendering this term a relevant conformal perturbation, and g has to be positive in order to fit numerical results.

Indeed, in a semiclassical analysis, the relevant third harmonic $-g \cos[3\sqrt{4\pi}\phi]$ is considered as a potential; it has three nonequivalent minima for the compactified boson field ϕ (see Fig. 3) signaling a threefold degenerate ground state. The mapping to spin variables, following the usual rule for magnetized systems,¹³ shows that each of the minima for ϕ corresponds to the so-called classical plateau states,¹² namely, up-up-down states related by lattice translations $i \rightarrow i+1, i+2$. This is just what numerical results⁹ show, a threefold degenerate ground state with spontaneous Z_3 symmetry breaking to states with up-up-down local magnetization structure. The denomination of classical plateau states indicates that these are essentially the states obtained in the Ising limit of the present spin system. Interestingly, this description is stable for a wide range of homogeneous variations of J_1 and J_2 couplings.

The second and third lines in Eq. (3) represent a modulated perturbation to the homogeneous zigzag ladder de-

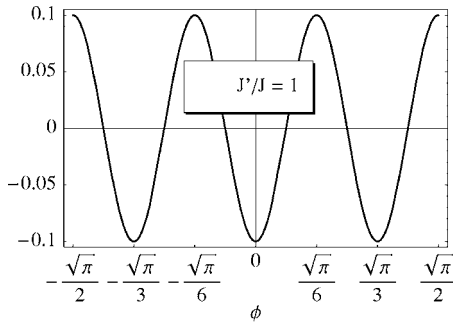


FIG. 3. Semiclassical potential for the homogeneous system $J = J'$ (in arbitrary units). There are three minima in the compactified range $(-\frac{\sqrt{\pi}}{2}, \frac{\sqrt{\pi}}{2})$, corresponding to the three nonequivalent up-up-down states.

scribed above. The key point in our presentation is that, after bosonization, these perturbations provide first and second harmonics in the Hamiltonian that are commensurate with the short scale oscillations given by $k_F = \pi/3$. Specifically, these terms yield an effective contribution which can be re-cast as

$$H_{mod} \sim \epsilon \int dx [C \cos(\sqrt{4\pi}\phi) - \cos(2\sqrt{4\pi}\phi)], \quad (5)$$

where C is a coefficient of order 3 ($C = 1 + \frac{2\pi}{3}$). These harmonics have smaller scaling dimensions than the third one, thus providing relevant perturbations that will compete with it. The presence of the first harmonic substantially modifies the theory. It is now the leading perturbation, and the effective-field theory $H_0 + H_{mod}$ is the so-called triple sine-Gordon model.¹⁴ Extensive analysis of competition between harmonics has been presented in Refs. 15–17, mainly focused on the double sine-Gordon model. The three-frequency case has been recently discussed in detail in Ref. 18.

Regarding spin systems, a model similar to ours has been recently analyzed by Hida and Affleck in Ref. 12, where a modulated perturbation on NN couplings of a zigzag ladder was proposed as a way to diminish frustration and enforce singlet formation on the $M=1/3$ plateau ground state. The effective theory obtained by these authors contains first and third harmonics of the bosonic field. In the present case, the second harmonics makes an extension of the above-mentioned results necessary.

We will first perform the semiclassical analysis of the ground state using the bare coefficients in Eq. (5). Thereafter, the renormalization-group (RG) flow of the relevant perturbations will be discussed.

For $J' > J$, the basic harmonic dominates the minimum of the potential (see Fig. 4, upper panel), so that the perturbation selects only one configuration $\phi=0$ corresponding to one of the up-up-down states out of the threefold degenerate ground state (the one with spins down on sites numbered by $3i+2$ in Fig. 1).

A richer scenario occurs for $J' < J$ when the first and second harmonics are in conflict with the triple harmonic term (see Fig. 4, lower panel). In this case, triple degeneracy is transformed first into double by an infinitesimal perturbation.

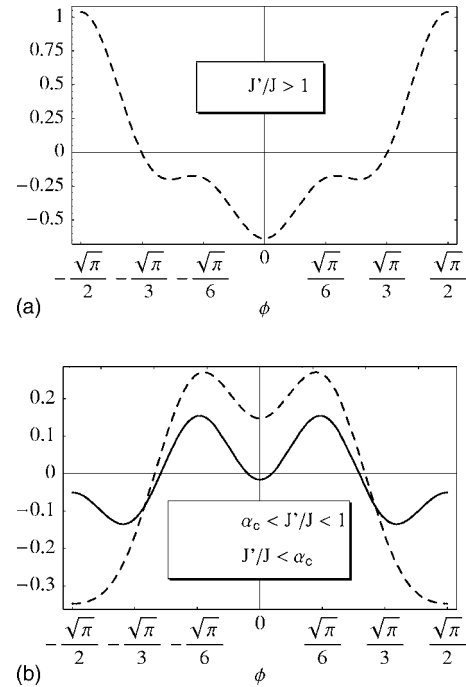


FIG. 4. Modification of the semiclassical potential by relevant harmonics (in arbitrary units). For $J' > J$ (upper panel), the single central minimum pins the system in a particular up-up-down state. For $J' < J$ (lower panel), the minimum structure takes the ground state first to double degeneracy and then, at some finite critical value of J'/J , to a single minimum shifted $\sqrt{\pi}/6$ with respect to nonperturbed position. This shift selects a quantum plateau state out of the triple degenerate up-up-down states.

From the three degenerate states at $J'=J$, it is precisely the state selected for $J' > J$, the one that now becomes excited, while the other two potential minima are selected and shifted from their commensurate up-up-down positions. This phase is characterized by Z_2 reflection symmetry, spontaneously broken by each of the potential minima. When $J-J'$ reaches some *finite* positive value, these two minima collapse into a single one at $\phi = \sqrt{\pi}/2 \equiv -\sqrt{\pi}/2$, lifting the degeneracy completely. Moreover, the position of the minimum is shifted to a commensurate field configuration which was a maximum for the homogeneous ladder. In terms of spins, the system is pinned in a very different configuration, the so-called quantum plateau state.¹² This configuration is characterized by spin singlets alternating with spin-up sites (in our case, with spin up at sites numbered by $3i+2$ in Fig. 1). Given the symmetries and degeneracy of the ground states on both sides of the critical point, one may conjecture that the transition belongs to the second-order Ising universality class.¹⁵

The preceding discussion describes the competition between harmonics, depending on the signs and values of their bare coefficients. The results are particularly sensitive to the relative coefficients of first and second harmonics. In order to describe the long-distance effective theory, the RG flow of the coefficients must be analyzed. To this aim, let us write the triple sine-Gordon Hamiltonian in a compact form as

$$H = H_{LL} + g_1 \cos(\sqrt{4\pi}\phi) - g_2 \cos(2\sqrt{4\pi}\phi) - g_3 \cos(3\sqrt{4\pi}\phi), \quad (6)$$

where H_{LL} is the free boson Hamiltonian (Luttinger liquid) with Luttinger parameter K . All the present cosine terms are relevant perturbations when $K < \frac{2}{9}$, and the signs have been chosen so as to represent the bare situation with positive coupling constants g_1 , g_2 , and g_3 . The region of parameters we are interested in corresponds to g_3 of order of unity, describing the homogeneous ladder Z_3 symmetric ground state, and small $g_1, g_2 \propto \epsilon$ describing the modulation effects. Up to second order in g_1 , g_2 , and g_3 , the perturbative RG equations read

$$\begin{aligned} \frac{d}{dl} \frac{1}{K} &= \frac{9\pi}{2} g_3^2, \\ \frac{dg_3}{dl} &= \frac{9}{8\pi} (2 - 9K) g_3, \\ \frac{dg_1}{dl} &= (2 - K) g_1 + \frac{13}{18} g_1 g_2 - \frac{5}{18} g_2 g_3, \\ \frac{dg_2}{dl} &= (2 - 4K) g_2 - \frac{4}{9} g_1 g_3, \end{aligned} \quad (7)$$

where l is the length scale. The first two equations are the well-known sine-Gordon RG equations;¹⁹ as expected, g_3 flows toward strong coupling and K decreases. The other two equations can then be solved using the solutions for K , g_3 . We performed a numerical analysis of Eqs. (7) in the region of interest. The typical form of the RG flow is shown in Fig. 5. The salient features are that g_1 remains positive and grows faster than g_3 , allowing for the modification of the semiclassical potential, and that in the perturbative regime g_2 remains positive and smaller than g_1 . This analysis proves that the phase transitions depicted above are correct in the low-energy (long-distance) renormalized effective theory.

We have then found that the bosonization analysis predicts a first-order phase transition at $J' = J$, as the configurations selected for ground states by the classical potential jump between different minima of the potential, and a second-order phase transition of Ising class at some finite value of $\alpha_2 = J'/J$, where two degenerate minima merge continuously into a single one.

A natural question now is if the quantum plateau phase remains stable for $J'/J < \alpha_2$. It is easy to see that there should be a further phase transition, as for $J'/J \ll 1$ the system is described by almost decoupled triangular trimers. We investigate this phase in the following section.

III. STRONG FRUSTRATION

In order to analyze the ground state of the system beyond the weak modulation regime, we choose in this section a different starting point, namely, the strong frustration regime. We consider the system as consisting of frustrated triangles of spin $S = \frac{1}{2}$ with antiferromagnetic exchange coupling J ,

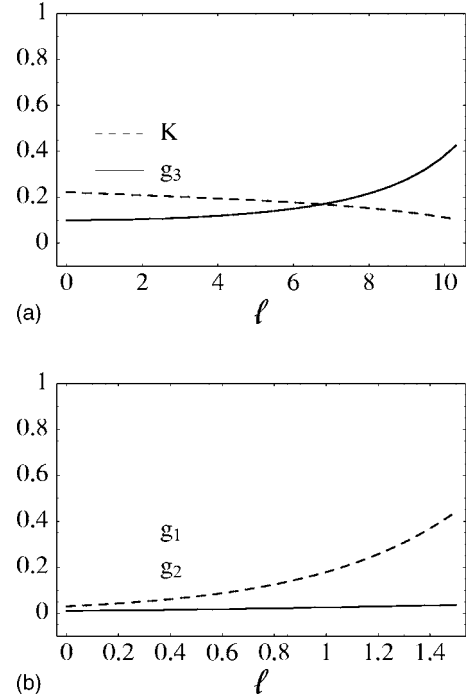


FIG. 5. Representative RG flow of triple sine-Gordon couplings in terms of the length scale. The region of interest is given by initial conditions $K < \frac{2}{9}$, $g_3 \gg g_2$, g_1 , and $g_1 = 3g_2$, corresponding to the bare Hamiltonian in Eqs. (4) and (5). (a) Couplings K and g_3 describing the homogeneous zigzag ladder. (b) First and second harmonics couplings g_1 and g_2 associated with modulated perturbations.

weakly coupled among them with exchange coupling $J' \ll J$. In this regime, the system can be thought of as a quasi-one-dimensional weakly coupled chain of triangles. The topology of weak couplings has been chosen so as to recover the zigzag chain in the limit $J'/J \rightarrow 1$, but similar systems with more symmetric intertriangle couplings have been considered in relation to spin tubes.²⁰ Notice that the $M = 1/3$ plateau is very robust for $J' \ll J$, as becomes apparent in the limit case $J' = 0$; we can then safely consider a plateau regime with $M = 1/3$ even for small magnetic fields.

For convenience, in this section, we enumerate the triangular trimers with an index n and rename spins as \vec{S}_n^a ($a = 1, 2, 3$ inside each trimer, see Fig. 6) to write the Hamiltonian in Eq. (2) as

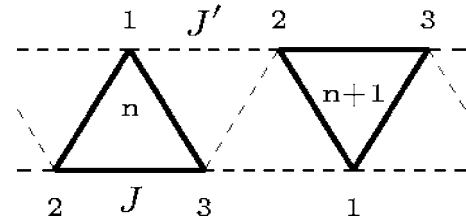


FIG. 6. Schematic description of the spin system in the strong frustration regime, with $J' \ll J$ as indicated by bold line trimers.

$$H = \sum_n J(\vec{S}_n^1 \cdot \vec{S}_n^2 + \vec{S}_n^2 \cdot \vec{S}_n^3 + \vec{S}_n^3 \cdot \vec{S}_n^1) + \sum_n J'(\vec{S}_n^1 \cdot \vec{S}_{n+1}^2 + \vec{S}_n^2 \cdot \vec{S}_{n+1}^3 + \vec{S}_n^3 \cdot \vec{S}_{n+1}^1). \quad (8)$$

We perform a systematic block-spin perturbative analysis^{21,22} around the highly degenerate exact ground state of the system of decoupled trimers ($J'=0$) at zero magnetic field. For low energy, the spin operators at each vertex can be factorized in terms of the triangle total spin operator and a pseudospin chiral operator²³ as

$$\vec{S}_n^a = \frac{2}{3}\vec{S}_{n,T} \left(\frac{1}{2} - T_n^a \right), \quad (9)$$

where

$$\vec{S}_{n,T} = \vec{S}_n^1 + \vec{S}_n^2 + \vec{S}_n^3 \quad (10)$$

is the total spin operator of the n th triangle projected onto the $S = \frac{1}{2}$ low-energy sector. Operators T_n^a act on a chiral sector as

$$T_n^1 = \tau_n^+ + \tau_n^-,$$

$$T_n^2 = \omega^2 \tau_n^+ + \omega \tau_n^-,$$

$$T_n^3 = \omega \tau_n^+ + \omega^2 \tau_n^-, \quad (11)$$

where τ_n^\pm are generators of the $S = \frac{1}{2}$ pseudospin sector, with $\tau_n^\pm = \frac{2}{\sqrt{3}}\vec{S}_n^1 \cdot \vec{S}_n^2 \wedge \vec{S}_n^3$, and $\omega = e^{i2\pi/3}$ a primitive cubic root of unity.

In order to study the $M=1/3$ plateau ground state, we consider the system under the action of an external magnetic field h^* high enough so as to force total magnetization $1/3$, but still low enough to discard excited spin states $S = \frac{3}{2}$ at any triangle. This regime is clearly available for small J'/J . The trimer spin degree of freedom is then saturated to $S_{n,T}^z = \frac{1}{2}$, leaving a pseudospin chain Hamiltonian describing nonmagnetic excitations. Notice that the magnetic field couples only to the total spin and plays no role in the pseudospin sector.

At first order in block-spin perturbations, we get a simple XY-like nearest trimer Hamiltonian,

$$H_{eff}^{(1)} = \frac{\sqrt{3}}{9} J' \sum_n (e^{-i\pi/6} \tau_n^+ \tau_{n+1}^- + e^{i\pi/6} \tau_{n+1}^+ \tau_n^-), \quad (12)$$

where we have dropped constant terms, including the magnetic field. One can perform a gauge transformation

$$\begin{aligned} \tau_n^+ &\rightarrow e^{-in\pi/6} \tau_n^+, \\ \tau_n^- &\rightarrow \tau_n^- \end{aligned} \quad (13)$$

that preserves SU(2) commutation relations to eliminate phases. Then, the usual Jordan-Wigner transformation maps nonmagnetic chiral excitations onto a gapless theory of free spinless fermions. The ground state is thus described by a half-filled fermion band.

From this effective model, one can also analyze the nonmagnetic excitations above the plateau ground state, which form a gapless continuum with nondegenerate ground state. Using Eqs. (10), (11), and (13), one can evaluate the ground-

state expectation value and correlations of spin operators. The spin density in the direction parallel to the applied field is uniform and simply equals average magnetization,

$$\langle S_n^z \rangle = 1/6, \quad (14)$$

whereas in-plane averages vanish. Equal-time spin-spin correlation function in the direction parallel to the applied field behaves as

$$\langle S_n^z S_m^z \rangle = \frac{1}{36} + \frac{\text{const}}{\sqrt{n-m}} \cos\left((n-m)\frac{\pi}{6} + \frac{2\pi}{3}(a-b) \right), \quad (15)$$

with $a, b=1, 2, 3$, and thus show long-range order (each triangle being in a spin $+1/2$ state) plus algebraically decaying oscillations. The in-plane-XY correlation functions decay exponentially. This picture is a consequence of the fact that nonmagnetic excitations are gapless, while magnetic excitations are gapped.

From the above discussion, one can state that for $J' \ll J$, the spin system at $M=1/3$ presents a gapless phase corresponding to nonmagnetic chiral degrees of freedom described by a Luttinger liquid with $K=1$.

In order to look for a quantum phase transition toward the quantum plateau state, it is necessary to construct the block-spin effective Hamiltonian at second order. This derivation requires a much longer calculation and provides next-nearest trimer interactions. Skipping details, once the total spin is saturated to $\frac{1}{2}$ at each triangle, we get for the second-order correction

$$\begin{aligned} H_{eff}^{(2)}/J = \alpha^2 &\left\{ \frac{2}{27} \sum_n [\tau_n^+ + \tau_n^-] \right. \\ &+ \frac{5}{162} \sum_n [e^{-i2\pi/3} \tau_n^+ \tau_{n+1}^- + e^{i2\pi/3} \tau_{n+1}^+ \tau_n^-] \\ &- \frac{1}{3} \sum_n \tau_n^\pm \tau_{n+1}^\pm \\ &+ \frac{2}{81} \sum_n [e^{i2\pi/3} \tau_n^+ \tau_{n+2}^- + e^{-i2\pi/3} \tau_{n+2}^+ \tau_n^-] \\ &- \frac{2}{27} \sum_n [\tau_n^+ \tau_{n+1}^+ + \tau_{n+1}^- \tau_n^-] \\ &\left. - \frac{4}{81} \sum_n [\tau_n^+ \tau_{n+1}^+ \tau_{n+2}^- + \tau_{n+2}^- \tau_{n+1}^- \tau_n^-] \right\}, \quad (16) \end{aligned}$$

where again we have dropped constant contributions. Terms in the second line are similar to those appearing at first order in Eq. (12), so we propose a different gauge transformation in order to eliminate the phase in XY terms,

$$\begin{aligned} \tau_n^+ &\rightarrow e^{i\lambda(\alpha)n} \tau_n^+, \\ \tau_n^- &\rightarrow \tau_n^-, \end{aligned} \quad (17)$$

where $\lambda(\alpha) = \arctan\left[\frac{\sqrt{3}(5\alpha-18)}{5\alpha+54}\right]$, rendering the total effective Hamiltonian written as

$$\begin{aligned}
H_{eff}/J = & -\rho(\alpha) \sum_n \left[\frac{1}{2} (\tau_n^+ \tau_{n+1}^- + \tau_{n+1}^+ \tau_n^-) + \Delta^z(\alpha) \tau_n^z \tau_{n+1}^z \right] \\
& + \frac{2}{81} \alpha^2 \sum_n [e^{-i2(\lambda(\alpha)-\pi/3)} \tau_n^+ \tau_{n+2}^- + \text{H.c.}] \\
& + \frac{2}{27} \alpha^2 \sum_n [e^{i\lambda(\alpha)n} \tau_n^+ + \text{H.c.}] \\
& - \frac{2}{27} \alpha^2 \sum_n [e^{i\lambda(\alpha)(2n+1)} \tau_n^+ \tau_{n+1}^+ + \text{H.c.}] \\
& - \frac{4}{81} \alpha^2 \sum_n [e^{i3\lambda(\alpha)(n+1)} \tau_n^+ \tau_{n+1}^+ \tau_{n+2}^+ + \text{H.c.}], \quad (18)
\end{aligned}$$

where $\Delta^z(\alpha) = \frac{\alpha^2}{3\rho(\alpha)}$ and $\rho(\alpha) = (\alpha/81) \sqrt{972 + 25\alpha^2}$.

In Eq. (18), the second and third lines represent an extended Heisenberg XXZ model with NN and NNN interactions for pseudospin operators. NN interactions have acquired the anisotropy parameter $\Delta^z(\alpha)$, while NNN interactions are XY -like, with a shifted band (because of the phase in the couplings); inspection of the coefficients shows that $0 < \Delta^z(\alpha) < 1$ and NNN couplings are small compared with NN ones. All the other terms include phases that depend on the position and will generally cancel out in the continuum limit, so that the continuous $U(1)$ symmetry broken by some of them is recovered. The low-energy behavior of this pseudospin $\frac{1}{2}$ model is then appropriately described by bosonization, where it is most clearly seen that oscillatory terms are incommensurate and can be neglected. We are essentially left with a one-dimensional spin $S = \frac{1}{2}$ anisotropic Heisenberg model.

Applying the standard bosonization procedure, we derive the low-energy Hamiltonian

$$H_{eff} \approx \frac{v}{2} \int dx \left[\frac{1}{K} (\partial_x \varphi)^2 + K (\partial_x \tilde{\varphi})^2 \right] - \Gamma \int dx \cos(2\sqrt{4\pi}\varphi), \quad (19)$$

where the Fermi velocity, the Luttinger parameter, and the coupling Γ depend on J'/J . For small J'/J , the harmonic perturbation is strongly irrelevant, so that the effective theory still describes a gapless phase. As J'/J increases, the conformal dimension of the harmonic perturbation decreases and one expects from Eq. (19) a second-order Brezinskii-Kosterlitz-Thouless (BKT)-like phase transition to a massive phase. A detailed computation allows us to estimate a critical value $J'/J \sim 0.5$, a value that is possible beyond the validity of block-spin perturbation theory.

IV. NUMERICAL ANALYSIS

In order to support the analytical results in the preceding sections and to explore the intermediate regime of J'/J not covered by perturbations around $J'=0$ and $J'=J$, we performed exact diagonalization analysis on finite systems with 12, 18, and 24 spins using periodic boundary conditions. However, in attempting to avoid misleading results in the

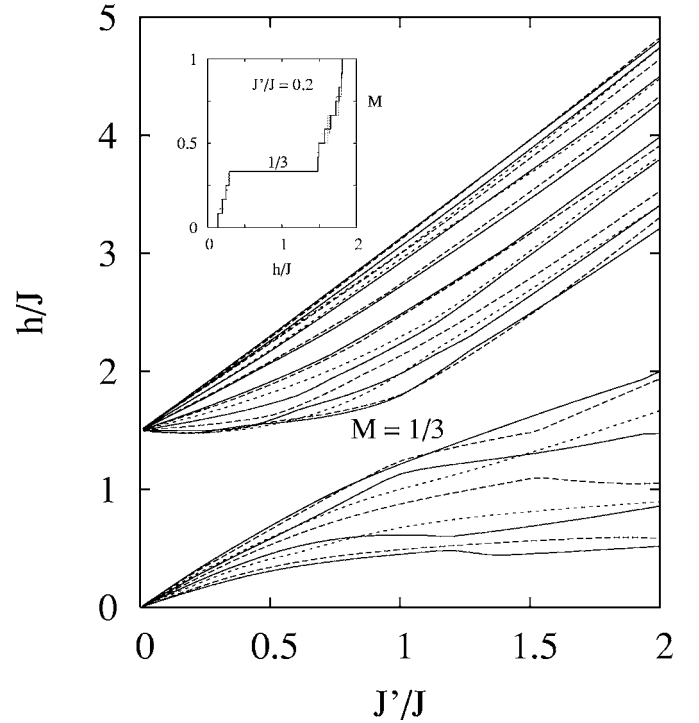


FIG. 7. Magnetic phase diagram obtained by exact diagonalization of finite system with 12 (dotted line), 18 (dashed line), and 24 (solid line) spins. Inset: a typical magnetization curve.

approximants and extrapolations referred to below, we discarded the 12 spin data.

We have first confirmed the presence of the $M=1/3$ magnetization plateau, all over the range from $J'=0$ to $J'=2J$. The magnetic phase diagram showing the magnetic field h necessary for level crossing between available magnetizations in several finite-size systems is presented in Fig. 7. A noticeable finite increment in h separates magnetic excitations from the $M=1/3$ ground state, indicating the magnetization plateau. This is interpreted to remain in the infinite-size scaling limit.

We have then computed the ground state and first three excitation energies in the subspace of magnetization $M=1/3$ in a wide range of couplings $0 < J'/J < 1.5$. In Fig. 8, we plot the gaps to excited energies in terms of J'/J . The triple degeneracy of the zigzag ladder ground state is, within finite-size effects, qualitatively observed at point $J'/J=1$ in agreement with Ref. 9. Moreover, assuming that the ground state will become degenerate in the thermodynamic limit, our numerical data are compatible with the picture that the triple degeneracy is lifted to a unique ground state for $J'/J > 1$. It also seems to be partially lifted to double degeneracy for $J'/J \lesssim 1$, where one level rapidly separates but another gets closer to the ground state, and only then rises lifting the remaining degeneracy.

One can estimate the locations of the Ising and BKT transition critical points mentioned in Secs. II and III by considering the Callan-Symanzik β function developed in the context of phenomenological renormalization group by Roomany and Wyld.²⁴ This technique can handle situations in which the phase transition is not necessarily characterized

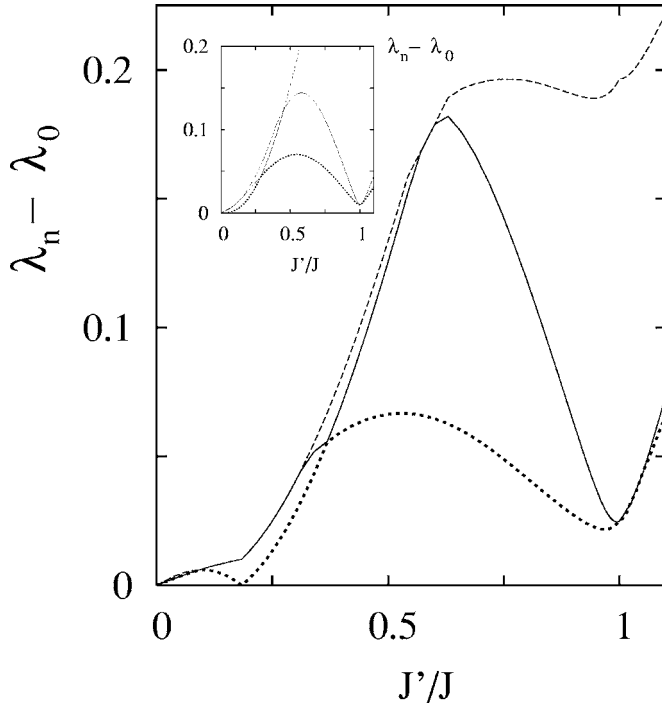


FIG. 8. Nonmagnetic excitations λ_n for 24 spins with periodic boundary conditions above the $M=1/3$ ground-state energy λ_0 for $n=1$ (dotted line), 2 (solid line), and 3 (dashed line). The inset shows the corresponding results for 18 spins. Numerical data in all subsequent figures were also obtained fixing $M=1/3$.

by a power-law decay of the spectrum gap, i.e., an ordinary second-order transition, but also by a singular BKT form. In the former case, the β function exhibits a simple zero, whereas in the latter situation, it vanishes with an algebraic singularity. This function can be estimated from finite lattice data by the Roomany-Wyld (RW) approximant, which in our notation reads

$$\beta_{\text{RW}}(\alpha) = \frac{\alpha \ln \left[\frac{N+6}{N} \frac{\Delta_{N+6}(\alpha)}{\Delta_N(\alpha)} \right]}{\ln \left(\frac{N+6}{N} \right) \left\{ 1 + \frac{1}{2} \alpha \partial_\alpha \ln \left[(N+6) \Delta_{N+6}(\alpha) N \Delta_N(\alpha) \right] \right\}}, \quad (20)$$

where Δ_N is the spectrum gap per spin. Notice that whenever the phenomenological renormalization condition $(N+6)\Delta_{N+6}(\alpha) = N\Delta_N(\alpha)$ is satisfied, the β function shows a zero. Furthermore, it behaves as $\beta(\alpha) \sim (\alpha - \alpha_c)/\nu$, from where the slope at α_c is related to the exponent of the second-order transition. Instead, in the vicinity of a singular transition of the form $\Delta \propto \exp -(\alpha - \alpha_c)^{-\sigma}$, one has $\beta \sim (\alpha - \alpha_c)^{1+\sigma}$, which ultimately determines both α_c and σ . In Fig. 9, we plot the RW approximant computed from 18 and 24 spin data. The leftmost curve characterizes a singular transition with $\alpha_1 \sim 0.35$ and $\sigma \sim 0.7$ (though not exhibiting a strict zero, possibly an artifact of our small lattice sizes), compatible with the BKT type, while the rightmost one typi-

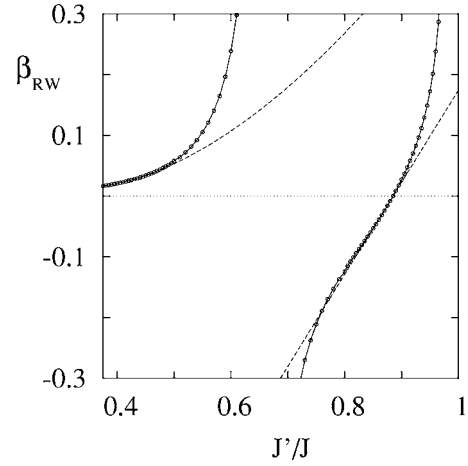


FIG. 9. The Roomany-Wyld approximant ($N=24, 18$) of the Callan-Symanzik β function (circles). The left and right curves are, respectively, consistent with a BKT phase transition at $\alpha_1 \approx 0.35$ and with an Ising transition at $\alpha_2 \approx 0.88$. Dashed curves fit the numerical data with the parameters referred to in the text.

fies a conventional transition at $\alpha_2 \sim 0.88$ with $\nu \sim 0.67$ consistent with the Ising class.

The BKT transition can also be estimated from level crossing spectroscopy²⁵⁻²⁷ of the low-lying states with different symmetries. In Fig. 10, we show the size-scaled excitation energies $N\Delta E(N)$ as functions of J'/J for finite-size clusters with $N=18$ and $N=24$ spins. The intersection between the first and second excitations is interpreted²⁶ as the chiral fluid-quantum plateau transition critical point $\alpha_1(N)$ and occurs at $\alpha = 0.29$ and $\alpha = 0.36$, respectively. The finite-size scaling of $\alpha_1(N)$ is expected to follow²⁵

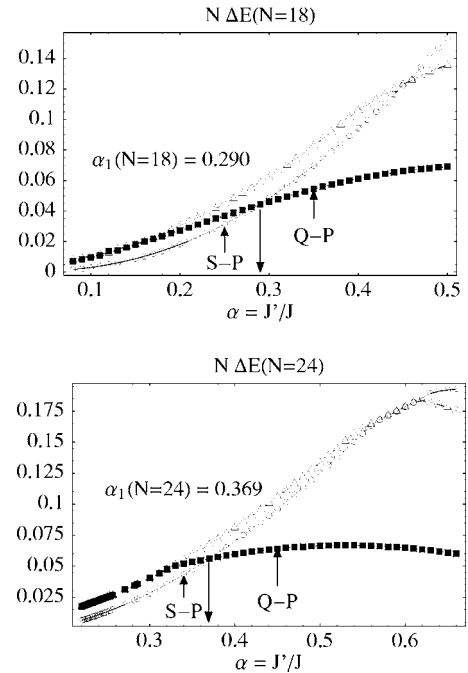


FIG. 10. Detail of scaled excited levels crossing used in the level spectroscopy analysis.

$$\alpha_1(N) = \alpha_1(\infty) + \text{const} \times N^{-2}, \quad (21)$$

suggesting a crude extrapolation to $\alpha_1(\infty) \approx 0.47$.

These numerical estimates are thus consistent with the existence of a BKT transition at α_1 in the range 0.3–0.5 and an Ising transition at α_2 around 0.9. However, a level crossing not predicted by the analytical treatment is seen in Fig. 8 at $J'/J \approx 0.18$ in the 24 spin system but not in the 18 spin one. Its presence should be checked in larger systems not currently available to us, as it may well be the consequence of highly oscillating terms in Eq. (18) which become particularly dominant for small lattice sizes. If confirmed, it would indicate that the BKT transition separating the gapless phase described in the strong frustration regime from the quantum plateau described in the weak modulation regime could be replaced by a first-order one in the thermodynamic limit. We cannot make a definite distinction from our current numerical data.

In order to characterize the phases separated by the mentioned transition points, we also computed the local magnetization profile for the ground state. We found three different periodic phases according to the generic J'/J values explored. As the profile is periodic, we report the configuration of a generic trimer, labeling sites $a=1,2,3$ in accordance with Fig. 6. A plot with local magnetization of the ground state for J'/J up to 1.4 is shown in Fig. 11 (upper panel). Notice that $a=2,3$ sites show the same magnetization.

In the strong frustration limit, we observe for the 24 spin system an almost uniform magnetized ground state for $0 < J'/J \leq 0.18$ (for instance, $S^{z1,2,3} = 0.018, 0.016, 0.016$ at $J'/J = 0.1$). In contrast, at intermediate regimes, we find a quantum-plateau-like magnetization for $0.18 < J'/J \leq 1$ (cf. $S^{z1,2,3} = 0.470, 0.015, 0.015$ at $J'/J = 0.5$), as well as an up-up-down magnetization for modulated regions $J'/J \geq 1$ (cf. $S^{z1,2,3} = -0.075, 0.288, 0.288$ at $J'/J = 1.2$). We find clear signals of a level crossing at $J'/J = 1$: the ground-state magnetization profiles correspond to a quantum plateau ($S^z \approx 0, 1/2, 0$ at each trimer) for $0.18 < J'/J \leq 1$ and up-up-down states [sign (S^z) = -, +, - at each trimer] for $J'/J \geq 1$. One can also appreciate a sudden magnetization change at the level crossing point $J'/J = 0.18$; the ground-state magnetization profile corresponds to uniform magnetization ($S^z \approx 0.166$ at each site) for $0 < J'/J < 0.18$ and to the quantum plateau for $0.18 < J'/J$. For the 18 spin system, the magnetization pattern is similar, except for the smooth behavior between the uniform magnetization and quantum plateau phases; this corresponds to the above-mentioned possibility of the transition being BKT-like instead of first order.

The numerical results can be summarized by an order parameter

$$M_s = \sum_i \cos\left(\frac{2\pi}{3}(i-2)\right) \langle S_i^z \rangle \quad (22)$$

describing a modulated local magnetization with period three. As shown in Fig. 11 (lower panel), this parameter allows the identification of three different phases. Notice that the second-order transitions, characterized by long-range fluctuations, are not expected to show up clearly in finite-size

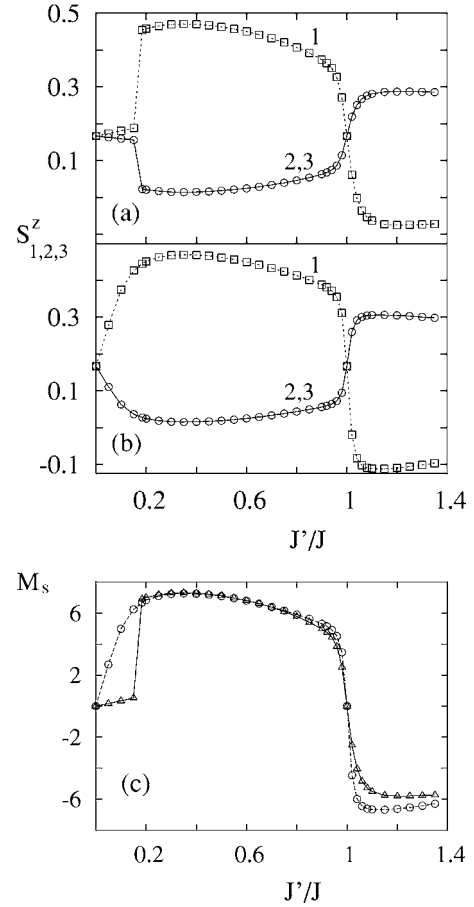


FIG. 11. Upper panel (a): local magnetization of the ground state of 24 spins as a function of the coupling parameter. Squares (circles) correspond to middle 1 (ending 2, 3) sites in trimers. Panel (b) displays, respectively, these results for 18 spins (here, the uniform phase is absent). Lower panel (c): order parameter in Eq. (22) describing modulated magnetizations for 18 (circles) and 24 (triangles) spins. From left to right, it exhibits uniform magnetization, quantum plateau, and up-up-down ground states.

systems. Thus, the results around $J'/J \leq 1$ are compatible with our previous semiclassical analysis.

As a separate issue, we have also tested the confidence of the first-order block-spin perturbation results. To this end, we computed the spectrum of the Hamiltonian obtained in Eq. (12), adapted to a finite-size system of 24 spins with periodic boundary conditions, through the Jordan-Wigner mapping to spinless fermions [care has to be taken in imposing periodic (antiperiodic) boundary conditions for odd (even) fermion filling to the resulting tight-binding Hamiltonian]. The spectrum thus obtained can be compared with exact Lanczos diagonalization of the full spin system at different values of J'/J . As it is known, the convergence of this method to highly excited states becomes progressively slow. To avoid this problem, we restarted the Lanczos procedure with an initial random state chosen orthogonal to each of the eigenlevels previously found. In Fig. 12, we plot in the upper panel the first excitations for $J'/J = 0.05$, showing very good agreement both in values and degeneracy of the energy levels. In the lower panel, the same is plotted for $J'/J = 0.2$,

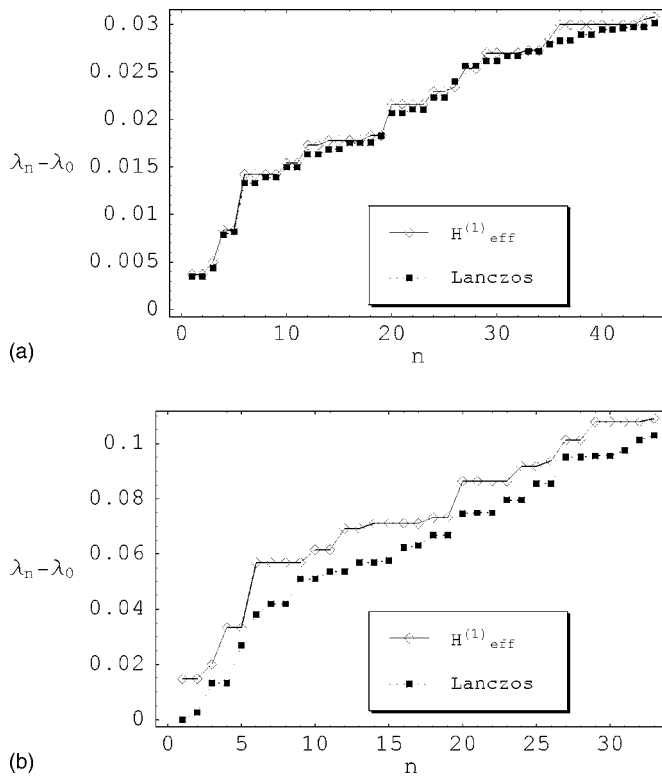


FIG. 12. Comparison of nonmagnetic excitations λ_n above the $M=1/3$ plateau, obtained on a finite system from the first-order block-spin perturbation and from exact diagonalization: (a) $J'/J = 0.05$ and (b) $J'/J = 0.2$. The horizontal and vertical axes are the excitation level (counting degeneracy) and $\lambda_n - \lambda_0$, respectively.

showing important deviations of the XY picture from the exact results. This deviation is expected because of the level crossing found numerically at $J'/J = 0.18$ in the 24 spin system.

V. SUMMARY AND CONCLUSIONS

In the present note, we have analyzed quantum phase transitions in zigzag antiferromagnetic spin $S = \frac{1}{2}$ ladders at

$M = 1/3$ driven by a trimerized modulation, as could be produced by adiabatic lattice deformations in a spin-Peierls-like transition.

Far from being stable, the triple degeneracy of the $1/3$ magnetization plateau in homogeneous ladders is lifted according to a triple sine-Gordon mechanism, giving place to several magnetic phases separated by first- and second-order transitions. Numerical diagonalization results in finite systems support our conclusions. A further transition separates the weak modulation regime from the strong frustration regime. From weak trimer coupling to beyond the homogeneous zigzag point, the phase diagram is schematically shown in Fig. 2: a phase with uniform magnetization described by nonmagnetic gapless chiral degrees of freedom, then a transition to a nondegenerate quantum plateau state, then a second-order transition, in the Ising universality class, to a twofold degenerate state, and finally a first-order transition at the homogeneous point to a nondegenerate up-up-down ground state. The nature of the transition between the chiral gapless phase and the quantum plateau is not resolved by our numerical data; we leave a blank in the phase diagram as an open question on this issue.

Motivated by the spin-Peierls transition usually studied at zero magnetization, it is interesting to investigate whether a lattice deformation such as the one analyzed in this work could take place at low temperatures in magnetized systems because of the competition between magnetic energy gain and elastic energy loss. We hope that the knowledge of the ground-state structure and nonmagnetic excitations presented here will be useful in such investigation. Related results will be published elsewhere.

ACKNOWLEDGMENTS

This work was partially supported by CONICET (Argentina), ECOS-Sud Argentina-France collaboration (Grant No. A04E03), PICS CNRS-CONICET (Grant No. 18294), PICT ANCYPT (Grant No. 20350), and PIP CONICET (Grant No. 5037). T.V. also acknowledges GNSF Grant No. N 06-81-4-100.

¹See, for instance, Table I in M. Hase, H. Kuroe, K. Ozawa, O. Suzuki, H. Kitazawa, G. Kido, and T. Sekine, Phys. Rev. B **70**, 104426 (2004).

²M. Hase, I. Terasaki, and K. Uchinokura, Phys. Rev. Lett. **70**, 3651 (1993).

³I. Affleck, in *Dynamical Properties of Unconventional Magnetic Systems*, NATO Advanced Studies Institute Series E: Applied Science (Kluwer Academic, Dordrecht, 1998), Vol. 349.

⁴E. Sorensen, I. Affleck, D. Augier, and D. Poilblanc, Phys. Rev. B **58**, R14701 (1998).

⁵G. Bouzerar, A. P. Kampf, and G. I. Japaridze, Phys. Rev. B **58**, 3117 (1998).

⁶A. Dobry and D. Ibaceta, Phys. Rev. B **59**, 8660 (1999).

⁷C. Knetter and G. S. Uhrig, Eur. Phys. J. B **13**, 209 (1999).

⁸T. Vekua, D. C. Cabra, A. Dobry, C. Gazza, and D. Poilblanc, Phys. Rev. Lett. **96**, 117205 (2006).

⁹K. Okunishi and T. Tonegawa, J. Phys. Soc. Jpn. **72**, 479 (2003).

¹⁰P. Lecheminant and E. Orignac, Phys. Rev. B **69**, 174409 (2004).

¹¹T. Tonegawa, K. Okamoto, K. Okunishi, K. Nomura, and M. Kaburagi, Physica B **346-347**, 50 (2004).

¹²K. Hida and I. Affleck, J. Phys. Soc. Jpn. **74**, 1849 (2005).

¹³See, for instance, D. C. Cabra and P. Pujol, in *Quantum Magnetism*, Lecture Notes in Physics Vol. 645 (Springer, Berlin, 2004).

¹⁴M. Høgh Jensen and P. S. Lomdahl, Phys. Rev. B **26**, 1086 (1982).

¹⁵G. Delfino and G. Mussardo, Nucl. Phys. B **516**, 675 (1998).

¹⁶M. Fabrizio, A. O. Gogolin, and A. A. Nersisyan, Nucl. Phys. B **580**, 647 (2000).

- ¹⁷Z. Bajnok, L. Palla, G. Takacs, and F. Wagner, Nucl. Phys. B **601**, 503 (2001).
- ¹⁸G. Z. Tóth, J. Phys. A **37**, 9631 (2004).
- ¹⁹See, for instance, T. Giamarchi, *Quantum Physics in One Dimension* (Clarendon, Oxford, 2004).
- ²⁰J.-B. Fouet, A. Lauchli, S. Pilgram, R. M. Noack, and F. Mila, Phys. Rev. B **73**, 014409 (2006).
- ²¹V. Subrahmanyam, Phys. Rev. B **52**, 1133 (1995).
- ²²F. Mila, Phys. Rev. Lett. **81**, 2356 (1998).
- ²³C. Raghunathan, I. Rudra, S. Ramasesha, and D. Sen, Phys. Rev. B **62**, 9484 (2000).
- ²⁴H. H. Roomany and H. W. Wyld, Phys. Rev. D **21**, 3341 (1980).
- ²⁵K. Okamoto and K. Nomura, Phys. Lett. A **169**, 433 (1992).
- ²⁶K. Okamoto and K. Nomura, J. Phys. A **27**, 5773 (1994).
- ²⁷K. Nomura, J. Phys. A **28**, 5451 (1995).
- ²⁸In our conventions, this ensures that the bosonized spin operators are single valued, as the compactification radius sets $\phi \equiv \phi + 2\pi R$. See, for instance, Ref. [13](#).